SAINSTEK: JURNAL SAINS DAN TEKNOLOGI
Publisher: Universitas Islam Negeri Mahmud Yunus Batusangkar
Website: https://ejournal.uinmybatusangkar.ac.id/ojs/index.php/sainstek
E-mail: sainstek@uinmybatusangkar.ac.id

June 2024
Vol 16 No 1
ISSN: 2085-8019 (p)
ISSN: 2580-278X (e)
pp : 45-50

Synthesis and Analysis of Activated Carbon Structure from Ketaping Fruit Shell Biomass Through X-Ray Diffraction Characterization

Rahma Joni[1]*, Hermansyah Aziz[2], Syukri[2]

[1]Chemistry Department, Universitas Lancang Kuning
Jl.Yos Sudarso KM. 8 Rumbai,Pekanbaru
[2]Chemistry Department, Universitas Andalas
Kampus Unand Limau Manis, Padang
**email: rahma.joni15@unilak.ac.id*

Article History
Received: 31 May 2024
Reviewed: 13 June 2024
Accepted: 20 June 2024
Published: 30 June 2024

Key Words
Activated carbon; X-ray Diffraction; Microcrystallite; Ketaping Fruit Shell.

Abstract
Synthesis of activated carbon from ketaping fruit shell biomass aims to produce high-quality active carbon to be applied in various fields. Activated carbon from ketaping fruit shells is synthesized by thermal treatment. It is synthesized through two stages, namely carbonation and activation. The carbonation stage is carried out at 400^{o}C under O_2 gas flow. This aims to break down lignol cellulose into carbon with low-quality pores through incomplete combustion. The activation stage is carried out by mixing activated carbon and KOH in varying ratios of 1:1, 1:3 and 1:5 wt. It is carried out by multilevel thermal treatment at 700^{o}C for 3.5 hours to form activated carbon with high pore quality. The activated carbon produced is then subjected to EDS characterization to see the active carbon content and XRD to see the structure of the active carbon with the characteristics of distance between layers, layer height, layer width, and number of layers. The results of EDX analysis show that the active carbon from the shell of the ketaping fruit contains 97.52% carbon and 2.48% oxygen. The results of XRD analysis show that the activated carbon surface area optimum at a molar ratio of 1:3 wt is 1,708.62 mg^{-1}. The distance of the resulting activated carbon layer is 0.3566nm at the 002 peak and 0.2102nm at the 100 peak. The layer height and width of the active carbon layer produced at a 1:3 wt ratio were 0.5489nm and 0.3002nm. Meanwhile, the number of layers of active carbon produced is 3 layers.

INTRODUCTION

Activated carbon is a promising material that has been studied extensively by several researchers. The application of activated carbon in society has been widely used in various fields such as health, beauty, renewable energy and water purification (Kumar Mishra et al., 2024). Activated carbon is widely used because it has a large surface area, cheap sample preparation, easy to obtain, has a high pore microstructure and has high conductivity (Spencer et al., 2024).

The production of activated carbon which is very easy to prepare is activated carbon which comes from biomass (Tetteh et al., 2024). Various studies have been carried out on the use of activated carbon, such as activated carbon from palm oil shells (Perdana et al., 2020), activated carbon from empty palm oil bunches

(Dwika Hardi et al., 2020), activated carbon from tea dregs (Mossfika et al., 2020), activated carbon from coffee dregs (Prabawati et al., 2023). In this research, ketaping fruit shells were used to synthesize activated carbon. The choice of ketaping fruit shells as a source of activated carbon is because it is easy to obtain, abundant and contributes to reducing organic waste (Dwika Hardi et al., 2020).

Increasing the maximum performance of activated carbon materials is by modifying the carbon pore structure. Micropore size is a good measure of improving the performance of activated carbon materials. Increasing the pore structure of activated carbon from biomass can be done in 2 ways, namely carbonization and activation. The carbonization process aims to enrich the carbon content in the percussion originating from the thermal treatment of lignocellulose and to remove the volatile content in the biomass so that low-quality carbon pores are formed(Spencer et al., 2024). The next process is the carbon activation process which is formed in the carbonization process, the activation process aims to impregnate the active substance into the activated carbon to form quality carbon pores. The active substances can be KOH (Mistar et al., 2020), NaOH (Mossfika et al., 2020), $ZnCl_2$ (Pimentel et al., 2023), H_3PO_4 (Neme et al., 2022), and H_2SO_4 (Neolaka et al., 2021).

The quality of the activated carbon produced depends on the amount of carbon and structure produced. The amount of carbon contained in activated carbon can be determined using EDS(Perdana et al., 2020). The structure of activated carbon was analyzed using X-ray diffraction (XRD) characterization. In the first approach, the shape of the XRD diffraction pattern provides an idea of the order or level of disorder of the active carbon structure. Although the XRD diagram of activated carbon presents the characteristics of amorphous materials, the characteristics of activated carbon include the distance between layers, layer height, layer width, number of layers and surface area that can be calculated using XRD data (Basheer et al., 2023).

In this study, the author investigated the synthesis of activated carbon from ketaping fruit shell bomb mass which was activated with KOH at a ratio of 1:1, 1:3, and 1:5 wt at an activation temperature of 800^0C. The resulting activated carbon is then analyzed using XRD carterization to determine the distance between layers, layer height, layer width and number of layers.

METHOD

Sample preparation was carried out by cutting the ketaping fruit shells into small pieces and cleaning them. The clean ketaping fruit shells are dried and then placed in the oven at 110 ^{O}C. Dried ketaping fruit shells are carbonized at 400^{O}C for 4 hours. The carbon formed was crushed and sieved with a 400 mesh sieve. The sieved carbon is activated using KOH by soaking the carbon in KOH for 12 hours at a molar ratio of 1:1, 1:3, 1:5 %wt. After the carbon soaking process has been filtered and dried in an oven, it is then activated at an initial temperature of 800^{O}C with the principle of gradual heating for 3.5 hours. The activation process is carried out under N gas flow$_2$ with a flow rate of 5 ^{0}C/min. The activated carbon is washed with HCl to pH 7 to remove organic impurities (Perdana et al., 2020).

The resulting activated carbon was then characterized using EDS and XRD with sources CuKα at a wavelength of 0.154 nm for determine the crystallite structure of activated carbon. The carbon XRD results analyzed the distance between layers (d), layer height (Lc), layer width (La) and number of layers (Np) using equations 1, 2 and 3.

The distance between layers of activated carbon is calculated using the Bragg equation, while the height, width and number of layers are calculated using the Dybe-Scherrer equation

$$d = \frac{\lambda}{2 \sin \theta}$$

where d is the distance between layers, is the wavelength and is the angle of scattering of X-rays

$$Lc = \frac{0{,}9\ \lambda}{\beta \cos \theta_{002}}$$

$$La = \frac{1{,}94\ \lambda}{\beta \cos \theta_{100}}$$

where Lc is the expansion of diffraction lines that can be calculated with ½ FWHM data, is the wavelength, 002 is the angle of scattering of X-rays at peak 002 and 100 X-ray scattering angle at the peak of 100 (Basheer et al., 2023).

The surface area of activated carbon is calculated based on the results of microcrystalline analysis which is calculated based on the equation

$$SSA_{XRD} = \frac{2}{\rho_{xrd} \cdot Lc}$$

where ρ_{xrd} is X-ray density given by the formula $\rho_{xrd} = (d_{002(grafit)}/d_{002})\ \rho_{(grafit)}$. $d_{002(grafit)} =$ 0.33354 nm and $\rho_{(grafit)} =$ 2.268 gcm^{-3}

RESULT AND DISCUSSION

Synthesis of activated carbon is carried out in 2 stages, namely the carbonization stage and the activation stage. The results of carbonization can be seen in Figure 1 (a) and activation can be seen in Figure 1 (b). Figure 1(a) shows that the activated carbon particles still follow the shape of the ketaping fruit shell sample. This ketaping fruit shell biomass sample which contains lignocellulose, through the carbonization process has removed the volatile substances in the sample. Copy that, at this stage carbon has been formed through incomplete combustion using O_2 gas. The mechanism for carbon formation at this stage begins with the combustion of the precursor into small particles which occurs at a temperature of 150-400ºC (4). Combustion of the precursor includes the breakdown of hemicellulose groups into carbon fan breakdown of cellulose groups into carbon. This was then followed by breaking down the lignin groups contained in the lignocellulose samples. The carbonized samples were then crushed using a 400 mesh sieve. The purpose of this sieving is to obtain a large surface area and high pore quality during the activation process. The particle size of this 400 mesh sieve is 38 micrometers (Pimentel et al., 2023).

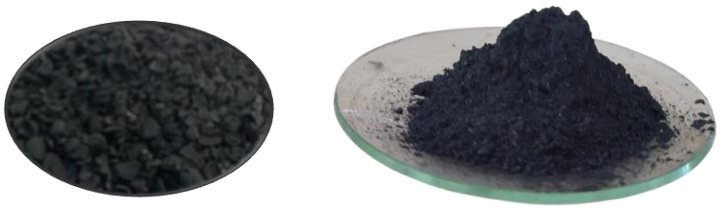

(a) (b)

Figure 1. Activated carbon in the carbonization and activation process

The second stage is the activation stage using KOH. The KOH activation stage aims to obtain high-quality carbon pores to maximize its application in various fields. The reaction mechanism of active carbon with KOH to remove K_2O, H_2 and K_2CrO_3. The K formed will be impregnated into the active carbon structure so that it will help the process of forming carbon pores (Mistar et al., 2020). The activated carbon produced is then subjected to EDS characterization to see the active carbon content and XRD to see the structure of the active carbon with the characteristics of distance between layers, layer height, layer width and number of layers.

Analysis of the amount of carbon produced in the synthesis of active carbon from the shell of the ketaping fruit can be seen in Figure 2.

The results of the EDX analysis shown in Figure 2 state that the percentage composition of the chemical elements contained in the active carbon from the shell of the ketaping fruit is carbon and oxygen (Dwika Hardi et al., 2020). From these results it can be seen that active carbon is the most abundant element in the active carbon sample from ketaping fruit shells, namely around 97.52%. This shows that the carbonization process of activated carbon is at a temperature of 400ºC obtained optimum conditions in breaking down the lignocellulose contained in the ketaping fruit shell samples. According to Taer et al. (2020) stated that the composition contained in activated carbon from biomass after activation is only the remaining carbon elements and a small percentage of oxygen remaining from incomplete combustion.

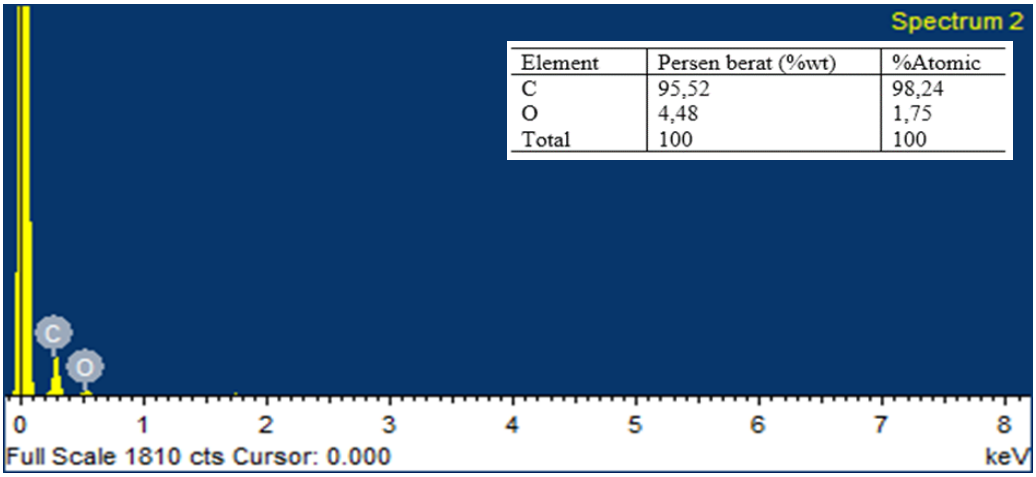

Figure 2. Analysis the amount of carbon produced

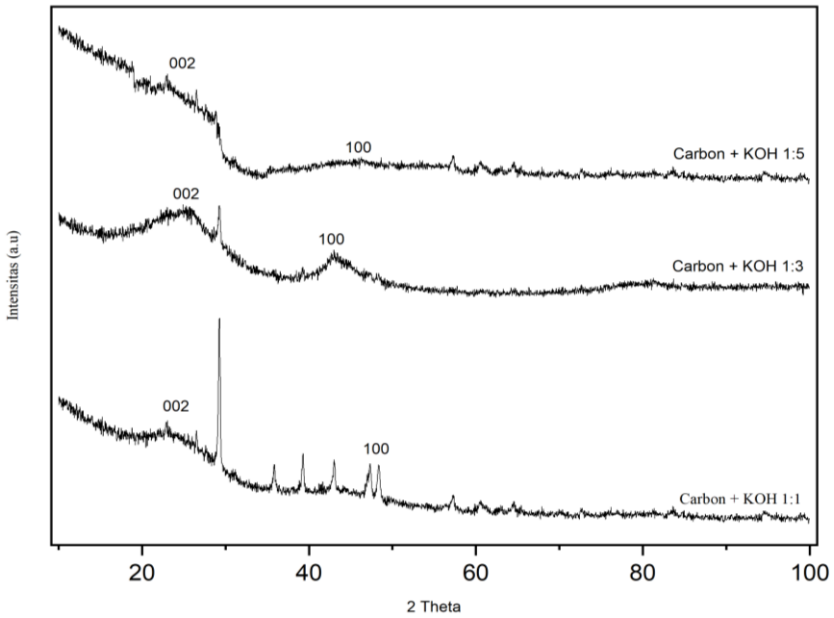

Figure 3. XRD analysis results

XRD analysis aims to see the structure of active carbon. Based on the results presented in Figure 3, it is clear that the active carbon structure is amorphous with 2 broad peaks. The structure of amorphous activated carbon is supported by research as reported by (Perdana et al., 2020). Apart from this, it is also based on the Joint Committee on Powder Diffraction Standards (JCPDS No. 75-1621). Based on the XRD analysis in Figure 2, the 1:3%wt ratio shows a diffraction pattern that is closer to the JCPDS pattern compared to the 1:1%wt and 1:5%wt ratios. The appearance of 2 broad peaks in the activated carbon sample from the shell of the ketaping fruit shells indicates that the XRD measurements aim to calculate the characteristics of the distance between layers, layer height, layer width and the number of active carbon layers. Peak 002 XRD data is used to calculate layer height and peak 100 XRD data is used to calculate layer width(Basheer et al., 2023).

The distance between microcrystallite layers is determined by the Bragg equation. The distance between the microcrystallite layers with a ratio of 1:3 %wt on the 002 plane is 0.3566 nm and in the 100 plane, it is 0.2102 as seen in Table 1.

Table 1. Characteristics of activated carbon

Ratio (%wt)	$2\theta_{002}$ (nm)	$2\theta_{100}$ (nm)	d_{002} (nm)	d_{100} (nm)	Lc (nm)	La (nm)	Lc/La (nm)	Np (nm)	SSA (m g^{-1})
1:1	29,2841	47,3281	0,3047	0,1919	24,4613	8,9538	2,7319	80,272	32,75376
1:3	24,9421	42,9861	0,3567	0,2102	0,5489	1,8285	0,3002	1,5388	1708,62
1:5	23,0441	57,3121	0,3856	0,1606	1,7363	1,9388	0,8956	4,5025	583,985

Table 1 also shows that the height of the microcrystalite layer Lc) of 1:3 %wt from the synthesis of ketaping fruit shells activated carbon is 0,5489 nm and the layer width (La) is 1,8285 nm. The Lc value is related to the surface area of the active carbon, where the greater the Lc value, the greater the surface area of the active carbon. The surface area of activated carbon with a ratio of 1;3 is greater than 1:1 and 1;5, namely 583,985 m g^{-1}. The number of layers (NP) of activated carbon microcrystallites was found to be 3 layers which contribute to the adsorption of ions or molecules according to their use.

CONCLUSION

Based on the research that has been carried out, it can be concluded that activated carbon from ketaping fruit shell biomass is synthesized through two stages, namely carbonation and activation. The carbonization stage was carried out at a temperature of 400ºC and the activation stage was carried out with multilevel thermal treatment at a temperature of 700ºC. Activated carbon from ketaping fruit shells only contains 97.52% carbon and 2.48% oxygen based on EDX results. The microcrystallite structure with a ratio of 1:3 %wt is more optimal in activating activated carbon compared to 1:1%wt and 1:5 %wt. The distance of the resulting activated carbon layer is 0.3566 nm at peak 002 and 0.2102 nm at peak 100. The layer height and width of the resulting active carbon layer are 0,5489 nm and 1,8285 nm. Meanwhile, the number of layers of active carbon produced is 3 layers based on the results of XRD analysis. The surface area of activated carbon based on microcrystallite analysis with a ratio of 1;3 is 1708.62 m g^{-1}.

REFERENCES

Basheer, A. O., Abu Odeh, A., & Al-Douri, Y. (2023). Structural analysis and characterization of date palm fiber-based low-cost carbon nanotubes and nanostructured powder activated carbon. *Heliyon*, *9*(8). https://doi.org/10.1016/j.heliyon.2023.e18811

Dwika Hardi, A., Joni, R., Aziz, H., Kimia Fisika, L., Kimia, J., & Artikel, H. (2020). Pembuatan Karbon Aktif dari Tandan Kosong Kelapa Sawit sebagai Elektroda Superkapasitor. *Jurnal Fisika Unand (JFU)*, *9*(4), 479–486. https://doi.org/10.25077/jfu.9.4.479-486-.2020

Kumar Mishra, R., Singh, B., & Acharya, B. (2024). A comprehensive review on activated carbon from pyrolysis of lignocellulosic biomass: An application for energy and the environment. In *Carbon Resources Conversion* (Vol. 7, Issue 4). KeAi Publishing Communications Ltd. https://doi.org/10.1016/j.crcon.2024.100228

Mistar, E. M., Alfatah, T., & Supardan, M. D. (2020). Synthesis and characterization of activated carbon from Bambusa vulgaris striata using two-step KOH activation. *Journal of Materials Research and Technology*, *9*(3), 6278–6286. https://doi.org/10.1016/j.jmrt.2020.03.041

Mossfika, E., Syukri, S., & Aziz, H. (2020). Preparation of Activated Carbon from Tea Waste by NaOH Activation as A Supercapacitor Material. *Journal of Aceh Physics Society*, *9*(2), 42–47. https://doi.org/10.24815/jacps.v9i2.15905

Neme, I., Gonfa, G., & Masi, C. (2022). Preparation and characterization of activated carbon from castor seed hull by chemical activation with H3PO4. *Results in Materials*, *15*. https://doi.org/10.1016/j.rinma.2022.100304

Neolaka, Y. A. B., Lawa, Y., Naat, J., Riwu, A. A. P., Darmokoesoemo, H., Widyaningrum, B. A., Iqbal, M., &

Kusuma, H. S. (2021). Indonesian Kesambi wood (Schleichera oleosa) activated with pyrolysis and H2SO4 combination methods to produce mesoporous activated carbon for Pb(II) adsorption from aqueous solution. *Environmental Technology and Innovation*, *24*, 101997. https://doi.org/10.1016/j.eti.2021.101997

Perdana, Y. A., Joni, R., Aziz, H., & Syukri. (2020). Effect of KOH Activator on the Performance of Activated Carbon from Oil Palm Kernel Shell as Supercapacitor Electrode Material. *J. Aceh Phys. Soc.*, *1*, 6–8. https://doi.org/10.16309/j.cnki.issn.1007-1776.2003.03.004

Pimentel, C. H., Díaz-Fernández, L., Gómez-Díaz, D., Freire, M. S., & González-Álvarez, J. (2023). Separation of CO2 using biochar and KOH and ZnCl2 activated carbons derived from pine sawdust. *Journal of Environmental Chemical Engineering*, *11*(6). https://doi.org/10.1016/j.jece.2023.111378

Prabawati, S. Y., Widiakongko, P. D., & Taqwim, M. A. (2023). Activated Charcoal from Coffee Dregs Waste as an Alternative Biosorbent of Cu(II) and Ag(I). *Indonesian Journal of Chemistry*, *23*(4), 1120–1128. https://doi.org/10.22146/ijc.83269

Spencer, W., Senanayake, G., Altarawneh, M., Ibana, D., & Nikoloski, A. N. (2024). Review of the effects of coal properties and activation parameters on activated carbon production and quality. In *Minerals Engineering* (Vol. 212). Elsevier Ltd. https://doi.org/10.1016/j.mineng.2024.108712

Taer, E., Natalia, K., Apriwandi, A., Taslim, R., Agustino, A., & Farma, R. (2020). The synthesis of activated carbon nanofiber electrode made from acacia leaves (Acacia mangium wild) as supercapacitors. *Advances in Natural Sciences: Nanoscience and Nanotechnology*, *11*(2). https://doi.org/10.1088/2043-6254/ab8b60

Tetteh, I. K., Issahaku, I., & Tetteh, A. Y. (2024). Recent advances in synthesis, characterization, and environmental applications of activated carbons and other carbon derivatives. *Carbon Trends*, *14*(February), 100328. https://doi.org/10.1016/j.cartre.2024.100328